**Journal FORTEI-JEERI**, Vol. 6, No. 2, November 2025: 95-105
https://jeeri.fortei.org/index.php/fortei-jeeri

# Analysis of The Impact of Cirata Floating PV Power Plant Integration On Frequency Stability In The 500 KV Java-Bali

**Yanuar Wahyu Gianto[1], Awan Uji Krismanto[2], Widodo Pudji Muljanto[3]**
*Department of Electrical Engineering, Institut Teknologi Nasional Malang[1,2,3]*
*Corresponding Author Email: yanuarwahyugianto@gmail.com

***Abstract*** -- The increasing demand for clean energy has accelerated the deployment of renewable energy sources, notably Solar Photovoltaic (PV) systems. The Cirata Floating Solar PV Plant, with an installed capacity of 192 MWp and interconnected to the 500 kV Java-Bali transmission network, represents a key national strategic project aimed at supporting the national energy mix target. However, the integration of inverter-based renewable generation such as PV plants introduces challenges to system frequency stability, primarily due to the absence of rotational inertia contribution. This study investigates the impact of the Cirata Floating Solar PV integration on the frequency stability of the 500 kV Java-Bali power system. The analysis is conducted through time-domain dynamic simulations using DigSILENT PowerFactory software, incorporating load flow and dynamic simulation methodologies under three operating scenarios: load shedding, 50% load Bekasi increase, and Tripping of saguling power plant. Key frequency stability indicators, namely frequency nadir and Rate of Change of Frequency (RoCoF), are evaluated. The simulation results indicate a degradation in frequency stability performance following the integration of PV due to reduced system inertia. Nevertheless, under specific operating conditions, the PV plant exhibits a beneficial damping effect on frequency deviations. Consequently, additional mitigation measures such as the deployment of energy storage systems or enhancement of spinning reserve are recommended to maintain adequate frequency stability in the power system.



DOI: 10.46962/forteijeeri.v6i2.38

***Keywords:***
PV Integration
Frequency Stability
Rate of Change of Frequency

***Article History:***
Received: May 22, 2025
Revised: November 27, 2025
Accepted: December 1, 2025
Published: December 1, 2025

## I. INTRODUCTION

Recently, the demand for clean and renewable energy has increased along with the increasing public awareness of climate change and its impact on the environment [1]. Solar Power Plants (PV PLANT) are one of the options for renewable energy. In Indonesia, floating solar power plants offer a unique approach to harnessing solar energy without requiring large amounts of land. The Cirata Floating Solar Power Plant is a national strategic project expected to make a significant contribution to increasing Indonesia's renewable energy capacity in order to achieve the 23% renewable energy mix target by 2025 [2]. This project is located at the Cirata Reservoir in West Java and is designed to generate environmentally friendly electricity with a substantial capacity.

However, the integration of floating solar power plants into the power transmission system presents its own set of challenges. One of the main challenges is maintaining frequency stability in the transmission system due to the intermittent nature of solar power generation [3]. Frequency stability is a crucial factor in maintaining the reliability and quality of power supply [4]. One of the key indicators of frequency stability in power systems is the Rate of Change of Frequency (RoCoF), which describes how quickly the system frequency fluctuates [5]. The RoCoF value will fluctuate when there is an imbalance between generated and consumed power, which affects the system's ability to stabilize itself [6]. By managing the balance between generator output and load, the frequency is maintained at its nominal level. With a standard limit of 4% of the nominal frequency, the system frequency must not fall below 48 Hz or rise above 52 Hz.

To analyze the effect of cirata floating solar power plant integration on frequency stability in 500KV Java-Bali electricity system using Power Factory DigSilent software. A study case of the 500 kV Java-Bali

power system will be simulated using a Load Flow and RMS Simulation methodology, accompanied by a comparative analysis of frequency response curves to evaluate frequency stability within the system. The objective of the simulations in this study is to assess the impact of load increase and the tripping of a synchronous generator on the frequency stability of the Java-Bali power system, both before and after the integration of the solar photovoltaic power plant.

## II. POWER SYSTEM STABILITY

In the transformation of modern energy systems, particularly with the increasing integration of Solar Power Plants (PV PLANT) and other Renewable Energy Sources (RES), power system stability analysis has become critically important. Power system stability refers to the ability of the system to maintain a balanced and steady-state operating condition following a disturbance, and to return to a new equilibrium state within an acceptable period of time.

The power system must continuously supply electricity at standard voltage and frequency levels and promptly restore normal operation in the event of any system disturbance[5].

An electric power system can be considered reliable if it meets the following criteria:

1. Reliability: The ability of the system to continuously supply power or energy without interruption.
2. Quality: The ability of the power system to maintain voltage and frequency levels within specified standards.
3. Stability: The ability of a system to return to normal operation after a disturbance.

Power system stability is a system characteristic that enables the synchronous machines' rotor movements to respond to disturbances during normal operation and to return to their original operating conditions once the system stabilizes [7].

Stability studies or analyses are generally classified into three types, depending on the characteristics and severity of the disturbance, as illustrated in Figure 1, namely:

1. Steady State Stability
2. Dynamic Stability
3. Transient Stability

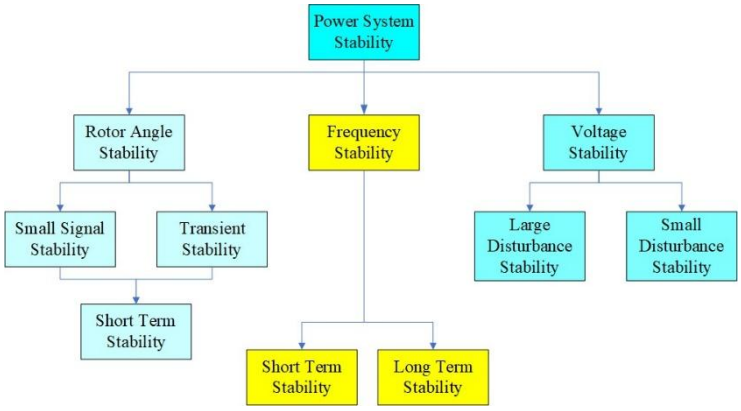


FIGURE 1.
Power System Stability

Steady-State Stability is the ability of the power system to maintain synchronization among generators following small disturbances, such as minor load variations. Dynamic stability refers to the capability of a power system to regain a stable operating point following large disturbances that persist for a significant duration. This form of stability analysis is more intricate, necessitating the consideration of the diverse components comprising the system.

Transient stability refers to the capability of a power system to maintain synchronism following severe disturbances, such as the sudden loss of a generator or significant and abrupt load variations[8]. Power system stability issues encompass frequency stability, voltage stability, and rotor angle stability. This classification is based on the temporal characteristics and underlying mechanisms of instability. Rotor angle stability is further subdivided into transient stability and small-signal stability. Small-signal stability pertains to the system's capability to damp electromechanical oscillations resulting from small perturbations, whereas transient stability arises from a loss of synchronizing torque due to large disturbances.

In this study, we utilized railway images categorized into two classes: defective and non-defective. The dataset originally consisted of three subsets: training, validation, and testing. The dataset employed in this study consists of a total of 384 rail surface images, distributed across training, validation, and testing subsets. The training set comprises 300 images, with an equal class distribution of 150 defective and 150 non-defective samples. For validation, 62 images are used, including 31 defective and 31 non-defective samples, ensuring balanced representation across both categories. The test set contains 22 images, equally divided into 11 defective and 11 non-defective cases. This balanced distribution of both classes ensured that the CNN models could learn discriminative features effectively.

### *A. Frequency Stability*

Deep Learning algorithms, such as Convolutional Neural Networks (ConvNet/CNNs), are able to Frequency stability is the capability of a power system to maintain or return its system frequency to a steady-state value following a disturbance that results in an imbalance between power demand and generation.

To continuously meet consumer electricity demand, a reliable power system must ensure a constant balance between power generation and system load. This equilibrium can be monitored through the system frequency. The maximum permissible frequency deviation specified by the system operator is typically ±4%, implying that all generating units connected to the grid must maintain synchronism within a frequency range of 48–52 Hz for a nominal 50 Hz system[9].

To ascertain the stability limits of the system, a systematic methodology and an accurate representation of its constituent components are necessary. Furthermore, it is crucial to comprehend the interaction of stability indices, such as the Rate of Change of Frequency (RoCoF) and frequency nadir, with key system parameters, such as kinetic energy.

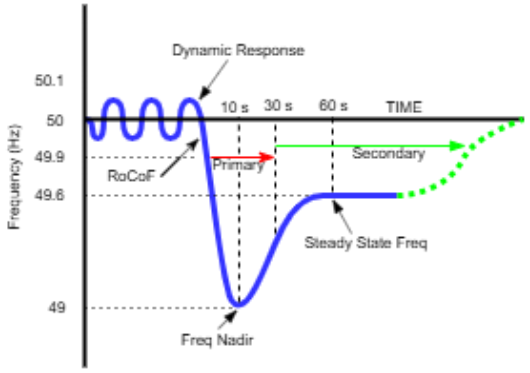


FIGURE 2.
Frequency Dynamic Response

Figure 2 illustrates the frequency response under a disturbance, where the power system frequency generally remains stable around 50 Hz but may drop due to sudden disturbances or rapid load changes. Both dynamic and non-dynamic response mechanisms operate to stabilize the system, with fast-acting (primary) control working to restore frequency toward its nominal value, followed by slower (secondary) control to ensure long-term stability and steady-state conditions.

### *B. Rate of Change of Frequency*

RoCoF (Rate of Change of Frequency) is a commonly used parameter in power systems to describe the rate at which frequency changes within the electrical grid [10].

Frequency stability in power systems is significantly influenced by the Rate of Change of Frequency (RoCoF), which serves as a key indicator for assessing the system's capability to maintain a stable frequency. Following a disturbance, such as an overload condition, the system frequency may decline. To restore nominal operating conditions, the frequency must be returned to its nominal value through either load shedding or an increase in power generation from synchronous generators.

The electric power system frequency is contingent upon the equilibrium between generated power and power consumption. Any disparity between these two quantities will impact the system frequency. The system frequency is required to remain within a standard tolerance of ±4% of the nominal value, implying that it must not fall below 48 Hz or exceed 52 Hz for a 50 Hz nominal system[11]. There is no universally defined and implemented RoCoF standard in Indonesia, nor is there one globally. For instance, Ireland and

Great Britain utilize a RoCoF standard of 0.25-0.4 Hz/s.

The system RoCoF value can be calculated using the following formula:

$$RoCoF(t) = \frac{DF(T)}{DT} \tag{1}$$

Where df(t) represents the frequency change at the n-th second (Hz), and dt is the time interval over which the frequency change occurs (s) [12].

## III. Dynamic Model

The dynamic machine model is used to analyze and understand the behavior of mechanical systems under dynamic conditions. The presented diagram represents the machine control system, involving various components and feedback loops.

### *A. Synchronous Machine*

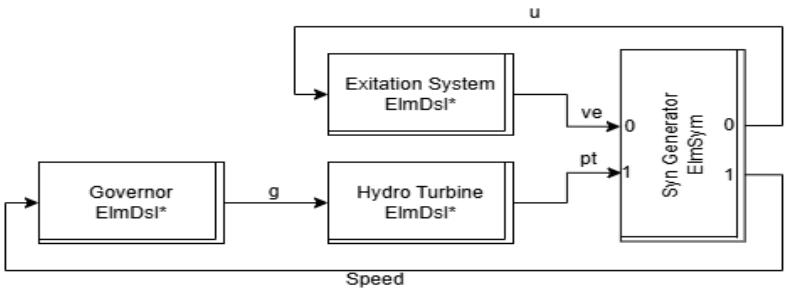


Figure 3.
Dynamic Model of Synchronous Machine

Figure 3 illustrates the minimal system of a power plant based on a synchronous generator. It comprises several functional blocks representing the synchronous generator, governor, turbine, and excitation system. The system operates such that the governor monitors the generator speed; upon deviation of the generator speed from the reference speed, the governor transmits a control signal to adjust the turbine gate position, thereby modulating the flow of the prime mover medium (water/steam) to the turbine. Concurrently, the excitation system monitors the generator terminal voltage and regulates the field excitation accordingly if the voltage deviates from the reference value.

### *B. Governor*

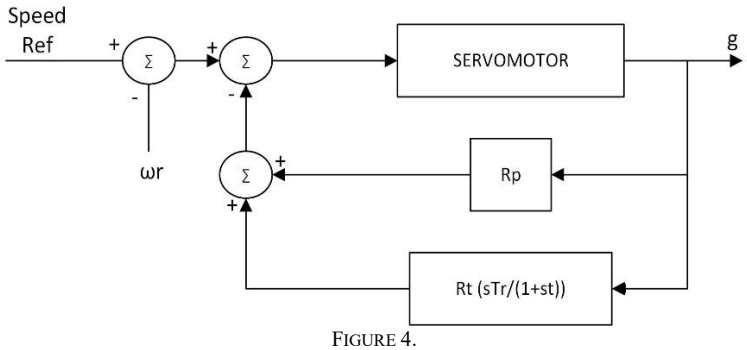


Figure 4.
Dynamic Model of Governor

Figure 4 illustrates the dynamic system of a governor that functions to regulate the machine speed (turbine speed control). The TP block represents the pilot valve and servo time constant. The [1/s] block is an integrator used to control the valve (gate) opening. Rp denotes the permanent droop, while RT and TR represent temporary droop and reset time, respectively. The governor continuously compares the reference speed with the actual machine speed. When a speed deviation occurs, the governor generates a signal to adjust the machine input (opening or closing the gate). Dynamic blocks such as the integrator and feedback loops help shape the governor response to be more stable, fast, and accurate. The droop allows stable operation of multiple generators, and the transient droop assists in enhancing stability during temporary

load changes.

*C. Auto Voltage Regulator (AVR)*

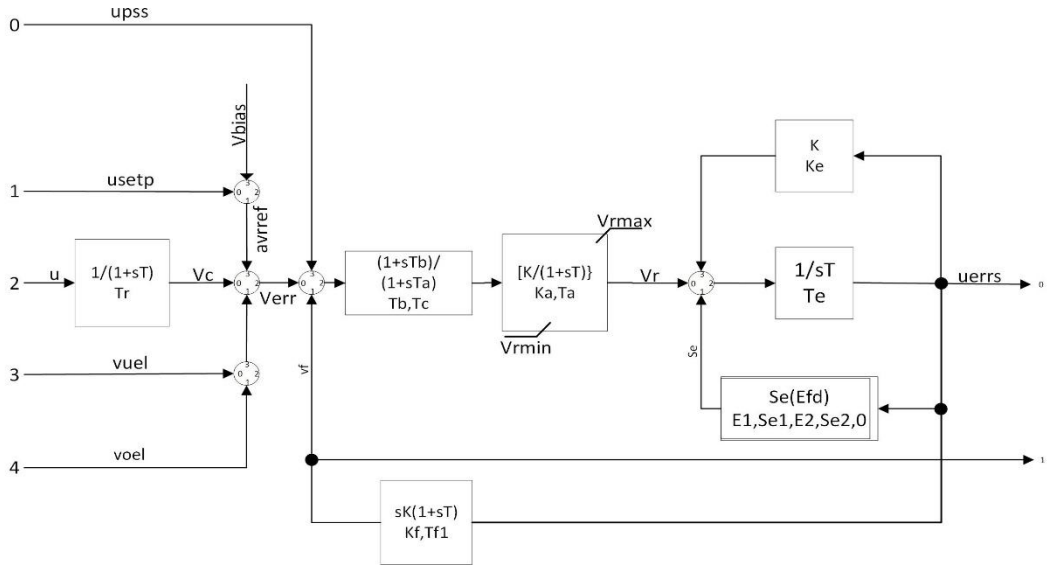


FIGURE 5.
Dynamic Model of AVR

Figure 5 illustrates the dynamic system of an Automatic Voltage Regulator (AVR), which functions to maintain the generator output voltage at the desired reference voltage. The AVR operates by measuring and comparing the generated voltage with the reference voltage (vreff - vmeas). The resulting voltage error is then used to control the generator excitation. Dynamic blocks such as the lead-lag compensator ((1+st1)/(1+st2)) and filter (1/(1+sTR)) are employed to ensure a stable and fast response. The exciter limiter (vuel, voel) is used to prevent over-excitation or under-excitation of the generator.

*D. PV Power Plants*

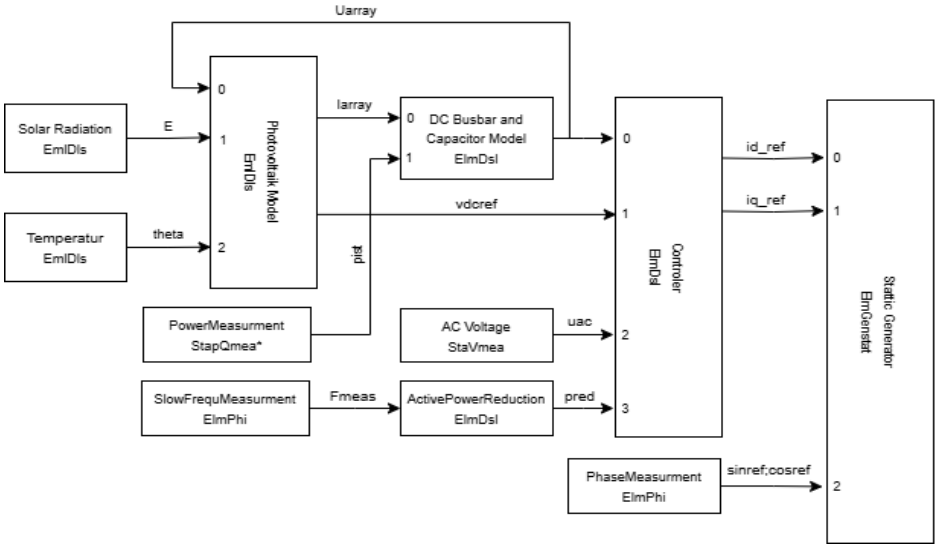


FIGURE 6.
Dynamic Model of PV Power Plants

Figure 6 illustrates the dynamic model of a solar PV system connected to the electrical grid. The Photovoltaic Model represents the solar panels with inputs of solar irradiance and temperature. The DC busbar and capacitor serve as the DC current connection point and act as voltage stabilizers and temporary energy storage between the PV and inverter. The controller block represents the control system that

regulates the inverter operation, while the Static Generator models the inverter that converts DC current into AC current suitable for grid requirements[13].

## IV. RESULT AND DISCUSSION

### *A. Cirata Reservoir Floating Solar Power Plants*

FIGURE 7.
Cirata Reservoir Floating Solar Power Plants

Floating solar PV (PV PLANT) is an innovative concept of installing solar power plants on water surfaces using floating technology. One implementation is the Cirata Floating Solar PV located in Citaminang, Manis District, Purwakarta Regency, West Java. With a capacity of 145 MW AC (equivalent to 192 MWp) and occupying a 200-hectare reservoir area, this PV PLANT is among the largest in Asia and operates on-grid, directly connected to the 500 kV Java-Bali transmission network.

### *B. Study Case*

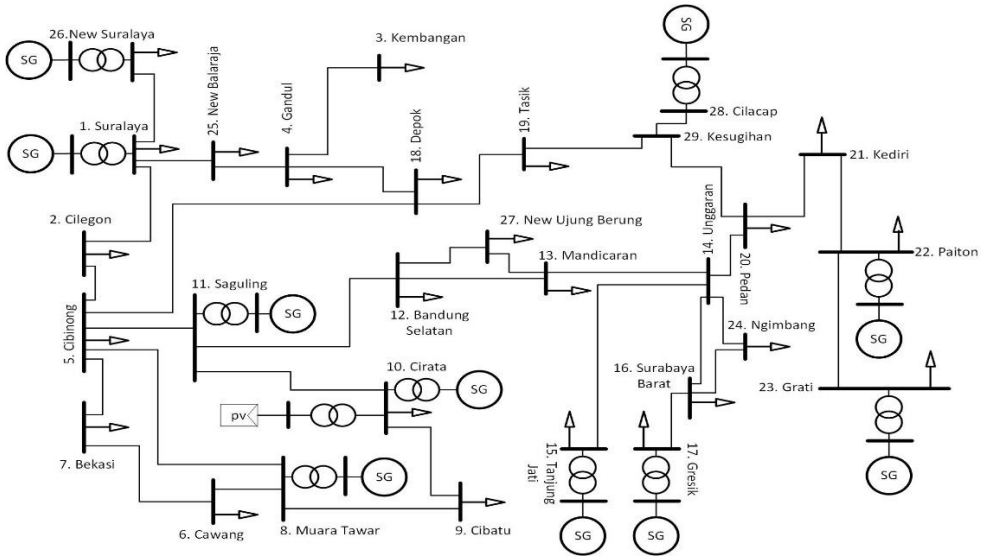


FIGURE 8.
Single Line Diagram of 500 KV Java-Bali

This study utilizes a single-line diagram of the 500 kV Java-Bali power system for simulation, employing DigSILENT PowerFactory 2015 software. To assess the system's frequency response, three distinct case studies will be conducted: a load increase at the Gresik load bus, load shedding at the Gresik load bus, and tripping of a conventional generator (Saguling Generator). Figure 8 depicts the single-line diagram of the 500 kV Java-Bali power system, which comprises 29 buses, 35 transmission lines, 1 slack bus, 9 generator buses, 24 load buses, and 1 solar PV plant.

*1) Load Increment*

A 50% load increment will be applied at the Bekasi load bus (Bus 7). The system's frequency response following this load increase disturbance will be monitored via the Muara Tawar generating unit (Bus 8), which is the closest generator to the disturbed bus.

Figure 9 illustrates the frequency response of the Muara Tawar generator during a 50% load increment at the Bekasi load bus from an initial load of 1196 MW, 9 MVAR, occurring at 40 seconds. The red line

represents the frequency condition without the Cirata solar PV plant, while the blue line represents the frequency with its integration. It can be observed that with the Cirata solar PV integration, the resulting transient is more pronounced than without it. Specifically, without the solar PV, the lowest frequency was 49.19 Hz at 47.9 seconds, whereas with the solar PV integration, the lowest frequency was 49.17 Hz at 47.9 seconds. The steady-state frequency without solar PV integration settles at 49.82 Hz at 74 seconds, whereas with solar PV integration, the steady-state frequency is 49.80 Hz at 74 seconds.

Table 1 presents a comparison of the frequency and Rate of Change of Frequency (RoCoF) values during the load increment. It's evident that with the Cirata solar PV integration, the final frequency, nadir frequency, and RoCoF are slightly worse than in the system without solar PV integration. The total active power generated by the system is shown in Table 2. It is evident that the power output from synchronous generators is slightly reduced when PV PLANT is integrated. This is because part of the power demand is supplied by the PV PLANT, which leads to a reduction in system inertia, making the system more vulnerable to frequency deviations.

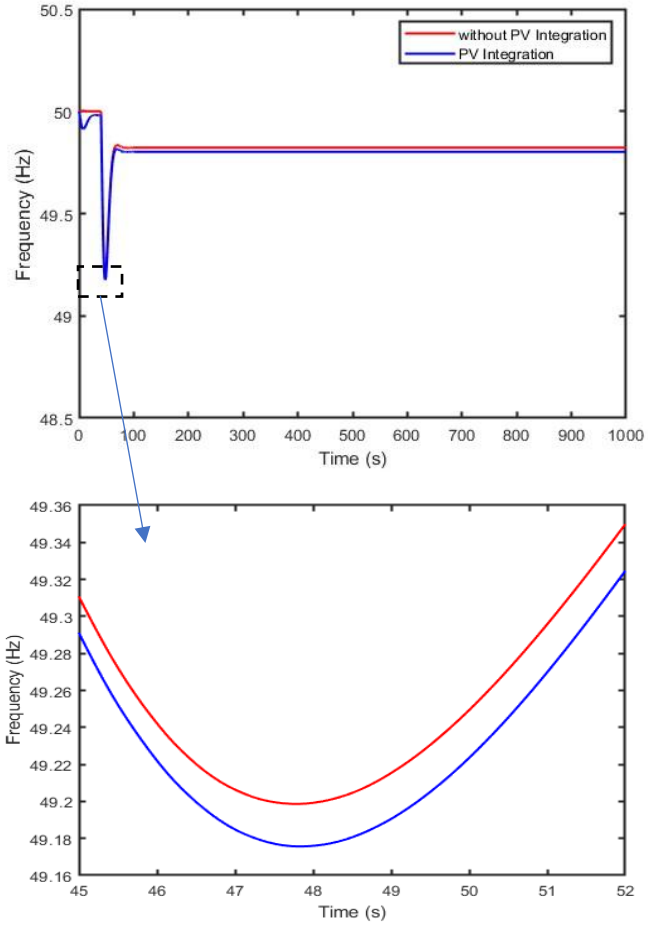


FIGURE 9.
Frequency Response and Nadir Frequency of Muara Tawar Generator (Bus 8)

TABLE 1.
Muara Tawar Generator Frequency Comparison

| Status | Frequency (Hz) | | RoCoF (Hz/s) | Nadir (Hz) |
|---|---|---|---|---|
| | *Initiall* | *Final* | | |
| Without PV Integration | 50 | 49,82 | -0,103 | 49,194 |
| PV Integration | 49,98 | 49,80 | -0,104 | 49,175 |

TABLE 2.
Total Synchronous Generator Output Comparison

| Status | *Active Power PV PLANT (MW)* | Total Generator Power Output | | Total Power Generation | |
|---|---|---|---|---|---|
| | | *Active Power (MW)* | *Reactive Power (Mvar)* | *Active Power (MW)* | *Reactive Power (Mvar)* |

| | | | | | |
|---|---|---|---|---|---|
| Without PV Integration | 0 | 12.389,8 | 3.982,52 | 12.389,8 | 3982,57 |
| PV Integration | 125,674 | 12.261,378 | 3864 | 12.387,05 | 3958 |

*2) Load Shedding*

Analysis of the frequency response of Generator 8 following the shedding of the 1196 MW, 9 MVAR load at the Bekasi bus is depicted in Figure.10 reveals that, without solar PV integration, the system experiences a transient starting at 40 seconds, rising from an initial frequency of 50 Hz to a peak frequency of 51.57 Hz at 47.8 seconds, and subsequently gradually decreasing to reach a steady-state frequency of 50.35 Hz at 79.2 seconds.Upon integration of the solar PV system, the frequency increases commencing at 40 seconds from an initial value of 49.98 Hz, attaining a peak frequency of 51.48 Hz at 47.6 seconds. Subsequently, the system frequency decreases until reaching steady-state conditions at 79.2 seconds with a frequency of 50.31 Hz.

Table.3 Shows the discrepancy in RoCoF observed in this experiment is approximately 0.01 Hz/s, with the RoCoF under non-integrated solar PV conditions registering a higher value of 0.20 Hz/s, while the RoCoF during solar PV integration is 0.19 Hz/s. A similar trend is evident in the peak frequency. In the absence of solar PV integration, the peak frequency attained is higher compared to the integrated scenario. This phenomenon arises because, during a sudden load rejection event, the proportion of generated power significantly exceeds the load demand, leading to a more rapid increase in the system frequency response. Conversely, with solar PV integration, the power output from conventional generators is inherently lower from the outset; consequently, when load rejection occurs, the frequency surge is less pronounced due to the initially reduced system inertia. Table 4 shows the comparison between the power output of the generator before and after the PV integration.

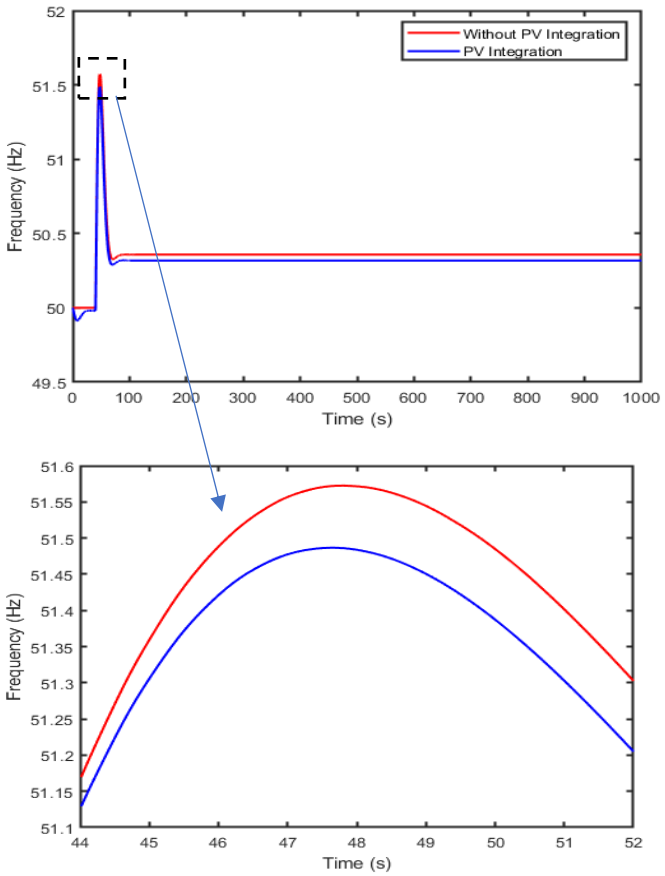


FIGURE 10.
Frequency Response Of Muara Tawar Generator (Bus 8) During Load Shedding

TABLE 3.
Muara Tawar Generator Frequency Comparison

| **Status** | **Frequency (Hz)** | | **RoCoF (Hz/s)** | **Spike (Hz)** |
|---|---|---|---|---|
| | *Initial* | *Final* | | |

| | | | | |
|---|---|---|---|---|
| Without PV Integration | 50 | 50,35 | 0,20 | 51,57 |
| PV Integration | 49,98 | 50,31 | 0,19 | 51,48 |

TABLE 4.
Total Synchronous Generator Output Comparison

| Status | Active Power PV (MW) | Total Generator Power Output | | Total Power Generation | |
|---|---|---|---|---|---|
| | | *Active Power (MW)* | *Reactive Power (Mvar)* | *Active Power (MW)* | *Reactive Power (Mvar)* |
| Without PV Integration | 0 | 10.607,53 | 3.696.32 | 10.607,53 | 3.696,32 |
| PV Integration | 60,8 | 10.543,998 | 3.591,8 | 10.604,81 | 3.685,11 |

*3) Conventional Power Plant Tripping*

Frequency response of the Cirata generating unit following the tripping of the Saguling generating unit is depicted in Figure.11 reveals that when the system is integrated with the solar PV, the frequency drops slightly further from its initial value compared to the system without solar PV integration. Similarly, for the steady-state frequency, the system with Cirata solar PV integration exhibits a slightly lower frequency than the system without it. Specifically, without solar PV integration, the final frequency is 49.81 Hz at 72.9 seconds, with the lowest frequency (frequency nadir) reaching 49.133 Hz at 47.9 seconds. In contrast, when integrated with the Cirata solar PV, the final frequency is 49.799 Hz, with the lowest frequency at 49.12 Hz.

Table 5 presents a comparison of frequency and Rate of Change of Frequency (RoCoF) values during the Saguling generator tripping event. It is evident that with Cirata solar PV integration, both the final frequency and frequency nadir are marginally worse compared to the system without solar PV integration. Table 6 illustrates the total active power generated by the system, clearly showing that the power output from synchronous generators is slightly reduced when the solar PV plant is integrated.

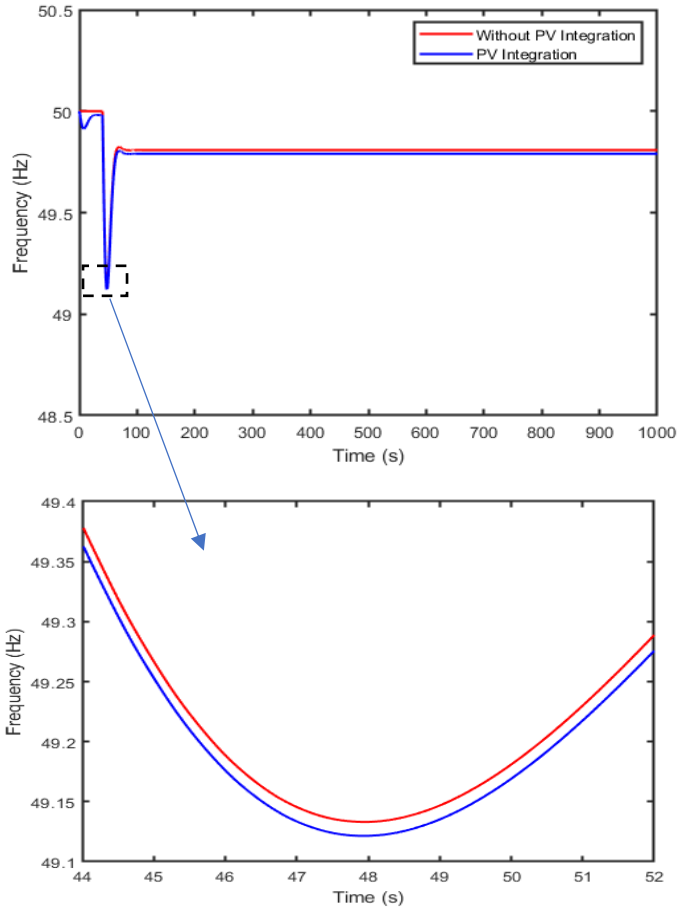

FIGURE 11.
Frequency Response Of Cirata Generator (Bus 10) During Generator 8 Tripping

TABLE 5.
Cirata Generator Frequency Comparison

| Status | Frequency (Hz) | | RoCoF (Hz/s) | Nadir (Hz) |
|---|---|---|---|---|
| | Initial | Final | | |
| Without PV Integration | 50 | 49,818 | - 0,109 | 49,133 |
| PV Integration | 49,98 | 49,799 | -0,108 | 49,121 |

TABLE 6.
Total Synchronous Generator Output Comparison

| Status | Active Power PV (MW) | Total Generator Power Output | | Total Power Generation | |
|---|---|---|---|---|---|
| | | Active Power (MW) | Reactive Power (Mvar) | Active Power (MW) | Reactive Power (Mvar) |
| Without PV Integration | 0 | 11.759,15 | 3957,10 | 11.759,15 | 3957,10 |
| PV Integration | 125.67 | 11.632,71 | 3.838,53 | 11.758,39 | 3.931,55 |

## V. CONCLUSION

Based on the findings of this study concerning the impact of Cirata floating solar PV integration on the frequency stability of the Java-Bali power system, the following conclusions were drawn:

1. The integration of the Cirata floating solar PV results in a reduction of system inertia, causing the system to become slightly more sensitive to frequency disturbances. This occurs because the integration of the solar PV replaces part of the generation from conventional power plants, thereby reducing overall system inertia. It is also reflected in the frequency response, which shows slight differences in the nadir frequency and RoCoF during disturbances, whether due to load increase or generator tripping.
2. In the 50% load increase scenario, the integration of the floating solar PV results in a lower frequency nadir compared to the system without solar PV (49.175 Hz versus 49.194 Hz), and a marginally higher Rate of Change of Frequency (RoCoF) (-0.104 Hz/s versus -0.103 Hz/s). This suggests that the system with solar PV integration exhibits increased vulnerability to disturbances owing to the diminished system inertia, as PV generation does not contribute to inertial response.
3. Load shedding events in the Java-Bali power system initiate a transient frequency increase. In the absence of the floating solar PV system, the frequency peaks at 51.57 Hz, while with solar PV integration, the peak frequency is reduced to 51.48 Hz. The post-transient steady-state frequency also exhibits a variation, registering 50.35 Hz without PV and 50.31 Hz with PV. The Rate of Change of Frequency (RoCoF) demonstrates a marginal decrease with the integration of PV. This phenomenon is primarily attributed to the significant surplus of generated power over load demand during load shedding, leading to the observed frequency rise.
4. When generator (Saguling) is tripped, the nadir frequency indicates that the system with Cirata solar PV integration experiences a slightly deeper frequency drop. However, it exhibits a marginally lower Rate of Change of Frequency (RoCoF), despite the difference being very small (RoCoF of -0.109 Hz/s without PV and -0.108 Hz/s with PV).

## VI. REFERENCE

[1] D. B. Anugraheni, "Akselerasi Net Zero Emissions Dengan Implementasi Energi Baru Terbarukan (EBT) Sebagai Bentuk Upaya Sustainable Development Goals (SDGs)," *Hubisintek*, vol. 1, no. 1, pp. 487–497, 2024, [Online].
Available: https://www.ojs.udb.ac.id/index.php/HUBISINTEK/article/view/3550

[2] Y. Pratama, Nofriyanto Eka Putra, and Atin Yudhi Wibowo, "Analisa Kuota Maksimum EBT Intermitten Pada Tahun 2025 Untuk Menjaga Kestabilan Frekuensi Di Sistem Sumatera," *J. Energi dan Ketenagalistrikan*, vol. 1, no. 1, pp. 30–36, 2023, doi: 10.33322/juke.v1i1.12.

[3] H. Bae, T. Tsuji, T. Oyama, and K. Uchida, "Frequency regulation method with congestion management using renewable energy curtailment," *IEEE Power Energy Soc. Gen. Meet.*, vol. 2016-

Novem, 2016, doi: 10.1109/PESGM.2016.7741811.
[4] B. S. Abdulraheem and C. K. Gan, "Power system frequency stability and control: Survey," *Int. J. Appl. Eng. Res.*, vol. 11, no. 8, pp. 5688–5695, 2016.
[5] R. Wahyu *et al.*, "Analisis integrasi pltb pada stabilitas frekuensi dalam jaringan kelistrikan sulbagsel berdasarkan rate of change of frequency 1, 2)," pp. 84–92, doi: 10.26623/elektrika.v16i2.10342.
[6] V. Z. Corina and M. Facta, "Analisis Kestabilan Frekuensi pada Mekanisme Pelepasan Beban Manual di Sub Sistem Kelistrikan Tanjung Jati," vol. 5, no. 4, 2016.
[7] S. Arbi, "Analisis Stabilitas Tegangan dan Frekuensi pada Microgrid AC Terhubung DG pada Mode Grid Connected dan Islanding," p. 94, 2017, [Online]. Available: http://repository.its.ac.id/44910/
[8] A. Hasibuan, "Analisis Stabilitas Sistem Tenaga Listrik Single Mesin Menggunakan Metode Runge Kutta Orde 4," *J. Elektro dan Telkomunikasi*, vol. Vol 4, no. No. 2, p. 24, 2017.
[9] M. Energi, D. A. N. Sumber, and D. Mineral, "Peraturan Menteri ESDM No. 37 Thn 2008 Grid Code Sumatera," pp. 1–184, 2008.
[10] S. Luitel and M. Karki, "Optimal Placement of Renewable Energy Resources to Minimize the Rate of Change of Frequency and Improve Frequency Nadir," pp. 827–831, 2023.
[11] A. Uji, "TRANSIENT FREQUENCY STABILITY ASSESSMENT OF THE INTERCONNECTED SOUTH SULAWESI POWER NETWORK," vol. 5, no. 2, pp. 63–67, 2024.
[12] E. Rakhshani, D. Gusain, V. Sewdien, J. L. Rueda Torres, and M. A. M. M. Van Der Meijden, "A Key Performance Indicator to Assess the Frequency Stability of Wind Generation Dominated Power System," *IEEE Access*, vol. 7, pp. 130957–130969, 2019, doi: 10.1109/ACCESS.2019.2940648.
[13] H. Setiadi, A. U. Krismantob, and N. Mithulananthan, "Influence of BES System on Local and Inter-Area Oscillation of Power System with.pdf," pp. 2–5, 2017.

## VII. BIOGRAPHIES

**Yanuar Wahyu Gianto** was born in Malang Regency on January 16, 2002 with an educational background at SMKN 6 Malang in 2017 majoring in Electrical Power Installation Engineering and graduated in 2020. Then continued his undergraduate studies at the National Institut Teknologi Nasional Malang with a concentration in Electrical Energy. The author is active in the activities of the Renewable Energy Laboratory assistant, Electrical Engineering Study Program S1 ITN Malang. The author's email is: yanuarwahyugianto@gmail.com